

Gamma Ray Bursts in the Swift-Fermi Era

Neil Gehrels^{1,*} and Soebur Razzaque^{2,†}

¹*Astrophysics Science Division, NASA Goddard Space Flight Center, Greenbelt, MD 20771 USA*

²*George Mason University, Fairfax, VA 22030, USA; Resident at Space Science Division,
Naval Research Laboratory, Washington, DC 20375 USA*

(Dated: December 11, 2013)

Gamma-ray bursts (GRBs) are among the most violent occurrences in the universe. They are powerful explosions, visible to high redshift, and thought to be the signature of black hole birth. They are highly luminous events and provide excellent probes of the distant universe. GRB research has greatly advanced over the past 10 years with the results from Swift, Fermi and an active follow-up community. In this review we survey the interplay between these recent observations and the theoretical models of the prompt GRB emission and the subsequent afterglows.

PACS numbers:

Contents

I. Introduction	1
II. Observations	2
A. Swift GRBs	2
B. Fermi GRBs	3
C. High redshift GRBs	4
D. GRB-Supernova connection	5
E. Short GRBs	5
F. Unusual GRBs and transients	6
III. Theory and Radiation Modeling	7
A. GRB fireball model	8
B. Prompt keV–MeV emission	8
C. Photospheric emission	8
D. Poynting flux dominated GRB model	9
E. GeV emission and plausible interpretations	9
F. GRB afterglow	11
G. High-energy neutrinos from GRBs	12
H. Gravitational waves from GRB	12
IV. Future GRB observations	12
V. Conclusions	13
VI. Acknowledgements	13
References	13

I. INTRODUCTION

GRBs are the most extreme explosive events in the Universe. The initial prompt phase lasts typically less than 100 s and has an energy content of $\sim 10^{51}$ ergs, giving a luminosity that is a million times larger than

the peak electromagnetic luminosity of a supernova. The GRB name is a good one because their spectra peak in the gamma-ray band between ~ 100 keV and ~ 1 MeV. The source of the energy powering the bursts is thought to be the gravitational collapse of matter to form a black hole or other compact object.

GRBs were discovered in the late 1960s by the Vela satellites monitoring the Nuclear Test Ban Treaty between the US and the Soviet Union [1]. It was slow progress for 20 years learning the origin of these brilliant flashes. Gamma-ray instruments of the time had poor positioning capability so only wide-field, insensitive telescopes could follow-up the bursts to look for counterparts at other wavelengths. Nothing associated with the GRBs was seen in searches hours to days after their occurrence. In the 1990's the Burst and Transient Source Experiment (BATSE) onboard the Compton Gamma Ray Observation (CGRO) obtained the positions of ~ 3000 GRBs and showed that they were uniformly distributed on the sky [2], indicating either an extragalactic or galactic-halo origin. BATSE also found that GRBs separate into two duration classes, short and long GRBs, with dividing line at ~ 2 s [3]. The detection of X-ray afterglows and more accurate localizations delivered by the BeppoSAX mission [4, 5] enabled optical redshifts of GRBs to be measured and their extragalactic origin to be confirmed. The long bursts were found to be associated with far-away galaxies at typical redshifts $z = 1 - 2$, implying energy releases in excess of 10^{50} ergs, after taking into account the jet beaming factor. The afterglow time decay often steepened after a day indicating a geometrical beaming of the radiation into a jet of opening angle $\sim 5^\circ$ [6].

Key open issues prior to the Swift and Fermi era included: (1) the origin of short GRBs, (2) the nature of the high energy radiation from GRBs, (3) the redshift distribution of bursts and their usage for early universe studies, and (4) the physics of the jetted outflows.

Swift and Fermi, launched in 2004 and 2008 respectively, have opened a new era in GRB research.

Swift is a NASA mission and Fermi a NASA collaboration with the US Department of Energy. They are both major international partnerships and have different

*Electronic address: neil.gehrels@nasa.gov

†Electronic address: srazzaqu@gmu.edu

and complementary capabilities. Swift has a wide-field imaging camera in the hard X-ray band that detects the bursts at a rate of ~ 90 per year, providing positions with arcminute accuracy. The spacecraft then autonomously and rapidly (100 s) reorients itself for sensitive X-ray and UV/optical observations of the afterglow. Fermi has two wide-field instruments. One detects bursts in the gamma-ray band at a rate of ~ 300 per year, providing spectroscopy and positions with 10-degree accuracy. The other observes bursts in the largely-unexplored high-energy gamma-ray band at a rate of ~ 10 per year. Combined, the two missions are advancing our understanding of all aspects of GRBs, including the origin of short bursts, the nature of bursts coming from the explosion of early stars in the universe and the physics of the fireball outflows that produce the gamma-ray emission.

II. OBSERVATIONS

A. Swift GRBs

The Swift mission [7] has three instruments: the Burst Alert Telescope (BAT; [8]), the X-Ray Telescope (XRT; [9]) and the UV Optical Telescope (UVOT; [10]). The BAT detects bursts and locates them to ~ 2 arcminute accuracy. The position is then sent to the spacecraft to repoint the XRT and UVOT at the event. Positions are also rapidly sent to the ground so that ground telescopes can follow the afterglows. There are more than 50 such telescopes of all sizes that participate in these world-wide follow-up campaigns. Measurements of the redshift and studies of host galaxies are typically done with large ground-based telescopes, which receive immediate alerts from the spacecraft when GRBs are detected. Swift has, by far, detected the largest number of well-localized bursts with afterglow observations and redshift determinations. As of 1 September 2012, BAT has detected 709 GRBs (annual average rate of ~ 90 per year). Approximately 80% of the BAT-detected GRBs have rapid repointings (the remaining 20% have spacecraft constraints that prevent rapid slewing). Of those, virtually all long bursts observed promptly have detected X-ray afterglow. Short bursts are more likely to have negligible X-ray afterglow, fading rapidly below the XRT sensitivity limit. The fraction of rapid-pointing GRBs that have UVOT detection is $\sim 35\%$. Combined with ground-based optical observations, about $\sim 60\%$ of Swift GRB have optical afterglow detection. There are 225 Swift GRBs with redshifts compared with 41 pre-Swift.

Swift was specifically designed to investigate GRB afterglows by filling the temporal gap between observations of the prompt emission and the afterglow [11]. Figure 1 shows example X-ray afterglows from XRT from long and short GRBs [12]. The combined power of the BAT and XRT has revealed that in long GRBs the non-thermal prompt X-ray emission smoothly transitions into the decaying afterglow. Often, a steep-to-shallow transition is

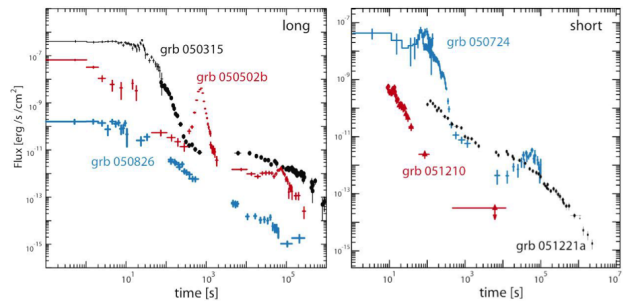


FIG. 1: Representative examples of X-ray afterglows of (a) long and (b) short Swift events with steep-to-shallow transitions (GRB050315, 050724), large X-ray flares (GRB050502B, 050724), and rapidly declining (GRB051210) and gradually declining (GRB051221a, 050826; flux scale divided by 100 for clarity) afterglows. From Gehrels, Ramirez-Ruiz and Fox (2009) [12].

found suggesting that prompt emission and the afterglow are distinct emission components [13, 14]. The early steep-decay phase seen in the majority of GRBs is a surprise. The current best explanation is that we are seeing high-latitude emission due to termination of central engine activity [14].

Swift has discovered erratic flaring behavior (Figure 1), lasting long after the prompt phase in $\sim 30\%$ of X-ray afterglows. The most extreme examples are flares with integrated power similar to or exceeding the initial burst [15]. The rapid rise and decay, multiple flares in the same burst, and cases of fluence comparable with the prompt emission, suggest that these flares are due to the central engine.

Long GRBs (LGRBs) are associated with the brightest regions of galaxies where the most massive stars occur [16]. LGRBs occur over a large redshift range from $z = 0.0085$ (GRB 980425) to $z > 8$ (GRB 090423 & GRB 090429B). With few exceptions, LGRBs that occur near enough for supernova detection have accompanying Type Ib or Ic supernovae. The exceptions are cases of bursts that may be misclassified as long or that may have exceptionally weak supernovae. These facts support the growing evidence that long bursts are caused by “collapsars” where the central core of a massive star collapses to a compact object such as a black hole [17] or possibly a magnetar [18, 19].

Theories for the origin of LGRBs predate Swift, but are supported by the new data. In them, a solar rest mass worth of gravitational energy is released in a very short time (seconds or less) in a small region of the order of tens of kilometers by a cataclysmic stellar event. The energy source is the collapse of the core of a massive star. Only a small fraction of this energy is converted into electromagnetic radiation, through the dissipation of the kinetic energy of a collimated relativistic outflow, a fireball with bulk Lorentz factors of $\Gamma \sim 300$, expanding out from the central engine powered by the gravitational accretion of surrounding matter into the collapsed core

or black hole.

B. Fermi GRBs

Mission & Statistics — The Fermi instruments are the Gamma-ray Burst Monitor (GBM, [20]) and the Large Area Telescope (LAT, [21]). The GBM has scintillation detectors and covers the energy range from 8 keV to 40 MeV. It measures spectra of GRBs and determines their position to $\sim 5^\circ$ accuracy. The LAT is a pair conversion telescope covering the energy range from 20 MeV to 300 GeV. It measures spectra of sources and positions them to an accuracy of $< 1^\circ$. The GBM detects GRBs at a rate of ~ 300 per year, of which on average 20% are short bursts. The LAT detects bursts at a rate of ~ 10 per year.

LAT bursts have shown two common and interesting features: (1) delayed emission compared to lower energy bands and (2) longer lasting prompt emission compared to lower energy bands. The four brightest LAT bursts are GRB 080916C [22], GRB 090510 [23, 24], GRB 090902B [25], and GRB 090926A [26]. They have yielded hundreds of > 100 MeV photons each, and together with the lower energy GBM observations, have given unprecedented broad-band spectra. In GRB 080916C, the GeV emission appears only in a second pulse, delayed by ~ 4 s relative to the first pulse (Figure 2). Such a delay is present also in short bursts, such as GRB 090510, where it is a fraction of a second. This soft-to-hard spectral evolution is clearly seen in all four of these bright LAT bursts, and to various degrees a similar behavior is seen in other weaker LAT bursts.

In some bursts, such as GRB 080916C and several others, the broad-band gamma-ray spectra consist of a simple Band-type broken power-law function in all time bins. In GRB 080916C the first pulse has a soft high energy index disappearing at GeV energies, while the second and subsequent pulses have harder high energy indices reaching into the multi-GeV range. In some other bursts, such as GRB 090510 [23, 24] and GRB 090902B [25], a second hard spectral component extending above 10 GeV without any obvious break appears in addition to common Band spectral component dominant in the lower 8 keV-10 MeV band.

An exciting discovery, unanticipated by results from the Energetic Gamma-Ray Experiment Telescope (EGRET) instrument on CGRO, was the detection of high-energy emission from two short bursts (GRB 081024B [27] and GRB 090510 [23, 24]). Their general behavior (including a GeV delay) is qualitatively similar to that of long bursts. The ratio of detection rates of short to long GRBs by LAT is $\sim 7\%$ (2 out of 27), which is significantly smaller than the $\sim 20\%$ by GBM.

While the statistics on short GRBs are too small to draw firm conclusions, so far, the ratio of the LAT fluence to the GBM fluence is $\sim 100\%$ for the short bursts as compared to $\sim 5\text{--}60\%$ for the long bursts. It is also note-

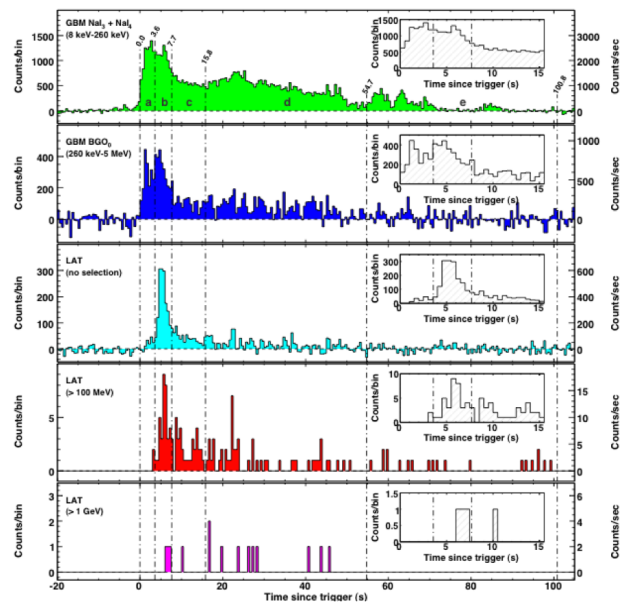


FIG. 2: Light curves of GRB 080916C with the GBM (top three panels) and LAT (bottom two panels). The high energy LAT emission is delayed relative to the lower energy GBM emission. From Abdo et al. 2009 [22].

worthy that, for both long and short GRBs, the $\gtrsim 100$ MeV emission lasts longer than the GBM emission in the < 1 MeV range. The flux of the long-lived LAT emission decays as a power law with time, which is more reminiscent of the smooth temporal decay of the afterglow X-ray and optical fluxes rather than the variable temporal structure in the prompt keV–MeV flux. This similarity in the smooth temporal evolution of the fluxes in different wave bands has been detected most clearly in GRB 090510 [28, 29] although this burst also requires a separate prompt component to the LAT emission [30]. This short burst was at $z = 0.9$, and was jointly observed by the LAT, GBM, BAT, XRT and UVOT.

The LAT detects only $\sim 10\%$ of the bursts triggered by the GBM which were in the common GBM-LAT field of view. This may be related to the fact that the LAT-detected GRBs, both long and short, are generally among the highest fluence bursts, as well as being among the intrinsically most energetic GRBs. For instance, GRB 080916C was at $z = 4.35$ and had an isotropic-equivalent energy of $E_{\text{iso}} \approx 8.8 \times 10^{54}$ ergs in gamma rays, the largest ever measured from any burst [22]. The long LAT bursts GRB 090902B [25] at $z = 1.82$ had $E_{\text{iso}} \approx 3.6 \times 10^{54}$ ergs, while GRB 090926A [26] at $z = 2.10$ had $E_{\text{iso}} \approx 2.24 \times 10^{54}$ ergs. Even the short burst GRB 090510 at $z = 0.903$ produced, within the first 2 s, an $E_{\text{iso}} \approx 1.1 \times 10^{53}$ ergs [24].

C. High redshift GRBs

Swift is detecting GRBs at higher redshift than previous missions due to its higher sensitivity and rapid afterglow observations. The average redshift for the Swift GRBs is 2.3 compared to 1.2 for previous observations. Although statistics are poor, the highest redshift GRBs are seen to have high luminosity, resulting in fluxes well above the detection threshold. Such bursts are also strong at other wavelengths. Table 1 presents optical data for the highest redshift GRBs observed to date. The optical brightness is given in magnitudes in R , I , J and K wavelength bands. The bursts are 3–4 orders of magnitude brighter than typical galaxies at these redshift.

To date, Swift has seen seven GRBs with $z > 5$. The highest z GRBs so far are $z = 6.3$ (GRB 050904 [31]), $z = 6.7$ (GRB 080913 [32]), $z = 8.2$ (GRB 090423 [33, 34]), and $z = 9.4$ (GRB 090429B [35]). Figure 3 shows a spectrum of the current record holder with a spectroscopic redshift, GRB 090423 [33]. Because GRBs are so bright across the electromagnetic spectrum, they are excellent tools for studying the high redshift universe. The information that can be provided by GRBs is complementary to what can be learned by studies of galaxies and quasars. For example, at $z > 8$ it is expected that the bulk of the star formation activity is taking place in small galaxies below the detection limits of HST.

The chemical evolution of the universe can be studied with GRBs as illustrated in Figure 4 [36]. GRBs provide data to higher redshift than active galaxies. The metallicity bias of GRBs is currently contradictory. Plots like Figure 4 show GRBs in higher metallicity star forming regions of galaxies. However, comparing star forming regions, GRBs actually tend to favor ones with lower metallicity [37].

Another way that GRBs are contributing to our understanding of the high-redshift universe is in the determination of the star formation history (Figure 5). LGRBs are the endpoints of the lives of massive stars and their rate is therefore approximately proportional to the star formation rate. They give information at high redshift where the rate is highly uncertain. There may be evolutionary biases, such as a dependence of LGRBs on the metallicity of host galaxies, so studies relating them to the star formation rate must include these factors into account [38, 39].

TABLE I: Optical Observations of High Redshift GRBs

z	t_{LB} (Gyr)	GRB	Brightness
9.4	13.1	090429B	$K = 19$ @ 3hr
8.2	13.0	090423	$K = 20$ @ 20 min
6.7	12.8	080913	$K = 19$ @ 10 min
6.3	12.8	050904	$J = 18$ @ 3 hr
5.6	12.6	060927	$I = 16$ @ 2 min
5.3	12.6	050814	$K = 18$ @ 23 hr
5.11	12.5	060522	$K = 21$ @ 1.5 hr

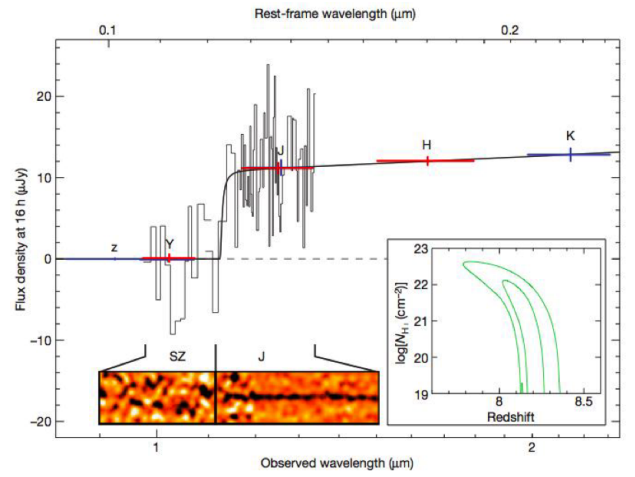


FIG. 3: The composite spectrum of the GRB 090423 afterglow obtained with the VLT. Also plotted are the sky-subtracted photometric data points obtained using Gemini North & South and VLT. A model spectrum showing the H I damping wing for a host galaxy with a hydrogen column density of $\text{NH I } 5 \times 10^{21} \text{ cm}^{-2}$ at a redshift of $z = 8.23$ is also plotted (solid black line). Inset, allowing for a wider range in possible host NH I values gives the 1σ (68%) and 2σ confidence contours shown. From Tanvir et al. 2009 [33].

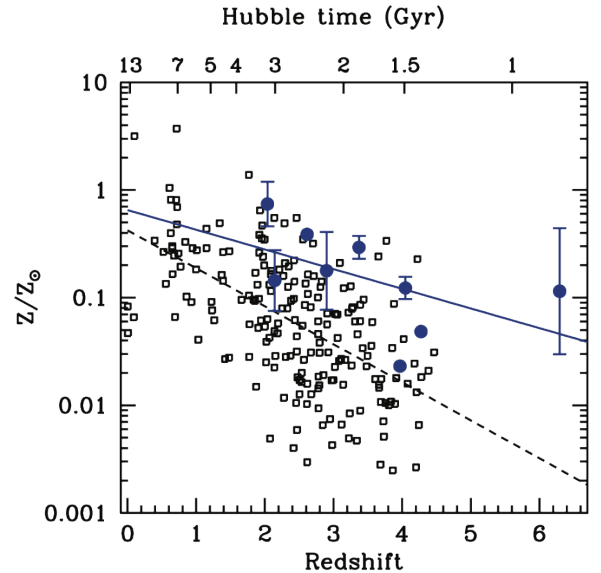


FIG. 4: Redshift evolution of the metallicity (represented here by the ratio of oxygen to hydrogen abundance) relative to solar values, for GRBs shown with blue dots and active galaxy quasars shown with open circles. The abundances are determined from spectral absorption lines in the continuum radiation. GRB lines are predominantly from the gas in the host galaxy in the star-forming region near the explosion, whereas quasars are of random lines-of-sight through the galaxy. The GRB metallicity is on average ~ 5 times larger than in QSO. These are based on damped Lyman alpha (DLA) spectral features. The upper horizontal x-axis indicates the age of the Universe (Hubble time). From Savaglio et al. 2006 [36].

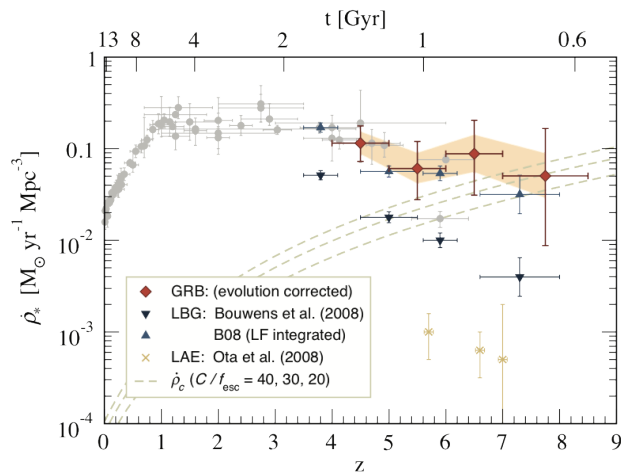


FIG. 5: Cosmic star formation history. Shown are the data compiled in Hopkins & Beacom [40] (light circles) and contributions from Ly emitters (LAE) [41]. Recent LBG data are shown for two UV LF integrations: down to $0.2L_*$ (down triangles; as given in Bouwens et al. [42]) and complete $z = 3$ (up triangles). Swift GRB-inferred rates are diamonds, with the shaded band showing the range of values resulting from varying the evolutionary parameters. Also shown is the critical density derivative from Madau et al. [43] for $C/f_{esc} = 40, 30, 20$ (dashed lines, top to bottom). From Kistler et al. 2009 [38]. See also study by Robertson & Ellis [39].

D. GRB-Supernova connection

On 18 February 2006 Swift detected the remarkable burst GRB 060218 that provided considerable new information on the connection between SNe and GRBs. It was longer (35 min) and softer than any previous burst, and was associated with SN 2006aj at only $z = 0.033$. SN 2006aj was a (core-collapse) SN Ib/c with an isotropic energy equivalent of a few 10^{49} erg, thus underluminous compared to the overall energy distribution for long GRBs. The spectral peak in prompt emission at ~ 5 keV places GRB 060218 in the X-ray flash category of GRBs [39], the first such association for a GRB-SN event. Combined BAT-XRT-UVOT observations provided the first direct observation of shock-breakout in a SN [44]. This is inferred from the evolution of a soft thermal component in the X-ray and UV spectra, and early-time luminosity variations. Concerning the SN, SN 2006aj was dimmer by a factor ~ 2 than the previous SNe associated with GRBs, but still ~ 2 – 3 times brighter than normal SN Ic not associated with GRBs [45, 46]. GRB 060218 was an underluminous burst, as were two of the other three previous cases. Because of the low luminosity, these events are only detected when nearby and are therefore rare. However, they are actually ~ 5 – 10 times more common in the universe than normal GRBs [47] and form a distinct component in the luminosity function [48].

GRB 060218 joins 4 other previous cases of GRBs from other missions that were associated with specific super-

novae (980425, 021211, 030329, 031203). In addition, there are several other Swift cases (050525A, 091127, 100316D, 101219B and 120422A). Table 2 gives a summary of all long GRBs that have had either specific supernovae or features in their afterglow lightcurves suggestive of the presence of a supernova. Many of the nearby GRBs with specific supernovae are in the underluminous class like GRB 060218. There are also a few cases listed in the table of nearby GRBs that had supernova searches, without a detection. Two of these, GRB 060505 and 060614 are discussed further in section II F.

TABLE II: Nearby GRBs and Supernova Detections or Limits

GRB	Redshift, z	Type ^a	SN Search
980425	0.0085	long-UL	SN 1998bw
020903	0.251	XRF-UL	LC bump & spectrum
021211	1.006	long-UL	SN 2002lt
031203	0.105	long-UL	SN 2003lw
030329	0.168	long	SN 2003dh
050525A	0.606	long-UL	SN 2005nc
060218	0.033	XRF-UL	SN 2006aj
091127	0.49	long-UL	SN 2009nz
100316D	0.059	long-UL	SN 2010bh
101219B	0.55	long-UL	SN 2010ma
120422A	0.283	long-UL	NS 2012bz
011121	0.36	long-UL	LC bump & spectrum
050826	0.297	long-UL	LC bump
060729	0.54	long-UL	LC bump
090618	0.54	long	LC bump
080120		long	LC bump GROND
081007		long	LC bump GROND
090424		long	LC bump GROND
100902A		long	LC bump GROND
110402A		long	LC bump GROND
040701	0.215	XRF-UL	no SN (< 0.1 SN98bw)
060505	0.089	“long”-UL	no SN (< 0.004 SN98bw)
060614	0.125	“long”	no SN (< 0.01 SN 98bw)
101225A	0.40	long	no SN (GCN 11522)

^aUL = underluminous, XRF = X-Ray Flash

E. Short GRBs

At the time of Swifts launch, the greatest mystery of GRB astronomy was the nature of short-duration, hard-spectrum bursts (SGRBs). Although more than 50 long GRBs had afterglow detections, no afterglow had been found for any short burst. In summer 2005 Swift and HETE-2, precisely located three short bursts for which afterglow observations were obtained leading to a breakthrough in our understanding of short bursts [49–55]. As of 2012, BAT has detected 65 SGRBs, 80% of which have XRT detections, and 15 of which have redshifts.

In contrast to long bursts, the evidence is that SGRBs typically originate in host galaxies with a wide range of star formation properties, including low formation rate. Their host properties are substantially different than

those of long bursts [56, 57] indicating a different origin. Also, nearby SGRBs show no evidence for simultaneous supernovae ([58]; and references therein), very different than long bursts. Taken together, these results support the interpretation that SGRBs arise from an old populations of stars and are due to mergers of compact binaries (i.e., double neutron star or neutron star - black hole) [58–60]. It is possible that there is a subpopulation of high-redshift, high-luminosity short GRBs with a different origin [61, 62].

Measurements or constraining limits on beaming from light curve break searches have been hard to come by with the typically weak afterglow of SGRBs. With large uncertainties associated with small number statistics, the distribution of beaming angles for SGRBs appears to range from $\sim 5^\circ$ to $> 25^\circ$ [65, 66], roughly consistent but perhaps somewhat larger than that of LGRBs. Swift observations also revealed long (~ 100 s) “tails” with softer spectra than the first episode following the prompt emission for about 25% of short bursts [67, 68]. Swift localization of a short GRB helps narrow the search window for gravitational waves from that GRB [69]. Detection of gravitational waves from a Swift GRB would lead to great scientific payoff for merger physics, progenitor types, and NS equations of state.

F. Unusual GRBs and transients

Here is a list of unusual transients detected by Swift [70].

Short GRB 050925: This unusual burst triggered the BAT with a single peaked outburst of duration $T_{90} = 70$ ms [71, 72]. It occurred near the galactic plane, and nothing was seen in the UVOT. However, the V -band extinction toward the source was $AV = 7.05$ mag. The XRT spectra and lightcurve show no significant X-ray emission in the field, suggesting that any X-ray counterpart to this burst was faint. Markwardt et al. (2005) [72] were able to fit a power law spectrum to the BAT data, with a photon index 1.74 ± 0.17 ; they found a better fit could be obtained with a blackbody spectrum $kT = 15.4 \pm 1.5$ keV, a value consistent with small-flare events from SGRs. The low galactic latitude and soft spectrum indicate a possible galactic source or SGR.

GRBs 060505 & 060614: GRB 060505 and GRB 060614 were nearby GRBs ($z = 0.089$ and 0.125 , resp.) with no coincident SN (Table 2), to deep limits [73]. GRB 060614 was bright (15–150 keV fluence of 2.2×10^{-5} erg cm^{-2}), and, with a T_{90} of 102 s, seemed to be a secure long GRB. Host galaxies were found [73–75] and deep searches were made for coincident SNe. All other well-observed nearby GRBs have had SNe, but GRB 060614 did not to limits > 100 times fainter than previous detections [72–74]. GRB 060614 shares some characteristics with SGRBs [68]. The BAT light curve shows an initial short hard flare lasting ~ 5 s, followed by an extended softer episode, ~ 100 s. The light curve is similar

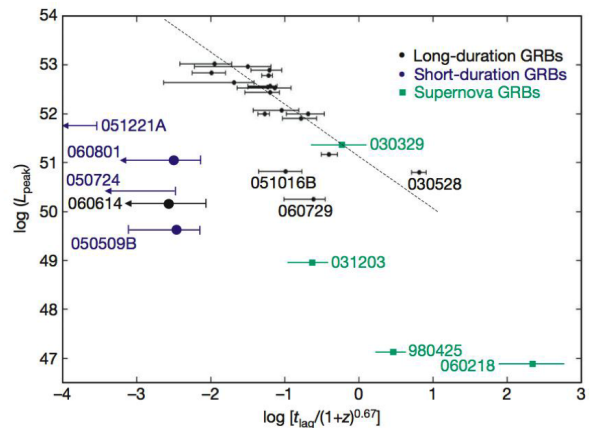


FIG. 6: Spectral lag as a function of peak luminosity showing GRB 060614 in the region of short-duration GRBs [68].

to some Swift SGRBs and a subclass of BATSE SGRBs [67]. GRB 060614 also falls in the same region of the lag-luminosity diagram as SGRBs (Figure 6). Thus GRB 060614 is problematic to classify. It is a LGRB by the traditional definition, but lacks an associated SN. It shares some similarities with SGRBs, but the soft episode is brighter, which would be difficult to account for in the NS-NS merger scenario.

Hostless GRB 070125: There is no obvious host galaxy for GRB 070125. Deep ground-based imaging reveals no host to $R > 25.4$ mag. Cenko et al. (2008) [76] present an analysis of spectroscopic data which reveals weak Mg II lines indicative of halo gas. In the field are two blue galaxies offset by $\gtrsim 27$ kpc at $z = 1.55$. If there is an association with one of them, it would imply a velocity $\sim 10^4$ km s^{-1} over a ~ 20 Myr lifetime of the massive progenitor. The only known way of achieving this would have been a prior close interaction with a massive BH. However, this interpretation was muddled by Chandra et al. (2008) [77], who inferred a dense environment, based on bright, self-absorbed radio afterglow. They proposed a scenario in which the high density material lies close to the explosion site, and the lower density material further away. They note GRB 070125 was one of the brightest GRBs ever detected, with an isotropic release of 10^{54} erg (by comparison, $M_\odot c^2 \approx 2 \times 10^{54}$ erg). The prompt emission from GRB 070125 was also seen by Suzaku/WAM [78].

Galactic GRB 070610: Discovered initially as GRB 070610, this object, now dubbed Swift J195509.6+261406 (Sw1955+26), is thought to represent a member of a relatively new class of fast X-ray nova containing a BH. It had a duration of ~ 5 s, and also shows large variability. Kasliwal et al. (2008) [79] discuss several possibilities for this source, and propose an analogy with V4641 Sgr, an unusual BH binary which had a major outburst in 1999 [80]. V4641 Sgr is a binary with a B9 III star orbiting a $\sim 9M_\odot$ BH [81] and also exhibited strong and fast X-ray and optical variability. The analog is imperfect in that

the normal star in Sw1955+26 is a cool dwarf rather than a B9 giant, suggesting a physical origin for the bursting behavior in the accretion disk and/or jet rather than the mass donor star. A ~ 5 s burst is certainly distinct from the \sim month long fast-rise exponential decay seen in systems like A0620-00 in 1975 [82, 83] which are thought to be due to a large scale storage and dumping of material in an accretion disk [84, 85], and may be more in line with either a disk-corona [86] or disk-jet instability [87]. Rea et al. (2011) [88] derive stringent upper limits on the quiescent X-ray emission from Sw1955+26 using a ~ 63 ks Chandra observation, and use this to argue against a magnetar interpretation. Simon et al. (2012) [89] present an analysis of optical emission during the 2007 outburst and find the optical emission manifests as spikes which decrease in duration as the burst progresses. They show that the emission can be explained by pure synchrotron emission. The main part of the optical outburst following the Swift/BAT trigger lasted ~ 0.3 d, with subsequent echo outbursts between 1 and 3 day, as in X-ray novae. The main part of the outburst has an exponential decay reminiscent of the 1975 outburst in A0620-00, but with a much shorter duration. If the global accretion disk limit cycle [84, 90] the mechanism for this outburst, it suggests a much shorter orbital period than the 7.75 hr for A0620-00 [91].

GRB 101225 Christmas burst: GRB 101225 was quite unusual: it had a $T_{90} > 1700$ s and exhibited a curving decay when plotted in the traditional $\log F$ - $\log t$ coordinates. The total BAT fluence was $\gtrsim 3 \times 10^{-6}$ erg cm^{-2} . The XRT and UVOT found a bright, long-lasting counterpart. Ground based telescopes followed the event, mainly in R and I , and failed to detect any spectral features. At later times a color change from blue to red was seen; HST observations at 20 d found a very red object with no apparent host. Observations from the Spanish Gran Telescopio Canarias at 180 d detected GRB 101225 at $gAB = 27.21 \pm 0.27$ mag and $rAB = 26.90 \pm 0.14$ [92]. Considered together, these characteristics are unique to this burst (Figure 7), and led Campana et al. (2011) [93] to propose that it was caused by a minor body like an asteroid or comet becoming disrupted and accreted by a NS. Depending on its composition, the tidal disruption radius would be $\sim 10^5$ – 10^6 km. Campana et al. find an adequate fit to the light curve by positing a $\sim 5 \times 10^{20}$ g asteroid with a periastron radius ~ 9000 km. If half the asteroid mass is accreted they derive a total fluence 4×10^{-5} erg cm^{-2} and distance ~ 3 kpc. Thöne et al. (2011) [92] offer a different explanation for GRB 101225 — the merger of a He star and a NS leading to a concomitant SN. They derive a pseudo-redshift $z = 0.33$ by fitting the spectral-energy distribution and light curve of the optical emission with a GRB-SN template. Thus in their interpretation the event was much more distant and energetic. They argue for the presence of a faint, unresolved galaxy in deep optical observations, and fit the long-term light curve with a template of the broad-line type Ic SN 1998bw associated with GRB 980425. If

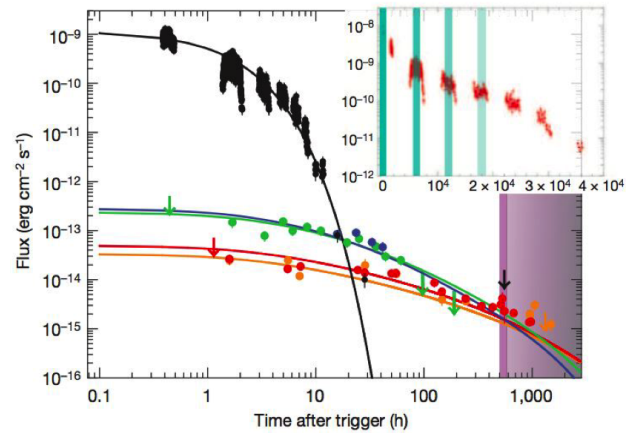


FIG. 7: Light curves of GRB 101225 in five energy bands: X-rays at 1 keV (black), UV at 2030 angstroms (green) and 2634 angstroms (blue), and optical at 6400 angstroms (R band, red) and 7700 angstroms (I band, orange) [93]. The inset (with t in seconds) shows the Swift/XRT light curve. Shaded regions highlight the periastron passages calculated using a tidal disruption model [93].

their distance is correct as well as their interpretation of a component emerging at 10 d as being a SN, then its absolute peak magnitude $MV_{abs} = -16.7$ mag would make it the faintest SN associated with a long GRB. The isotropic-equivalent energy release at $z = 0.33$ would be $> 1.4 \times 10^{51}$ erg which is typical of other long GRBs but greater than most other low-redshift GRBs associated with SNe.

III. THEORY AND RADIATION MODELING

Gamma-ray bursts are thought to be the endpoints of evolution of massive, $\gtrsim 30M_{\odot}$, stars (favorite for long GRBs) [12] or neutron star-neutron star/black hole close binaries (favorite for short GRBs) [58–60, 94]. In either case a black hole and a short-lived accretion disc are thought to be formed after the core collapse (long GRBs) or binary merger (short GRBs). In some cases a highly magnetized neutron star, called a magnetar, may form as an intermediate state which eventually collapses to a black hole [95]. Gravitational binding energy of the system is released within a short time scale which eventually produces the GRB phenomenon when some fraction of the gravitational energy converts to gamma rays. This is done via accretion of material/gas onto the black hole.

The compact core of a few solar mass with the Schwarzschild radius $r_g \sim 10^6 (M_{BH}/3M_{\odot})$ cm forms the central engine of a GRB. Infalling gas onto the newly-formed black hole is accreted with high efficiency. Most of the gravitational energy, $\sim 10^{54}$ ergs, is radiated in ~ 10 MeV thermal neutrinos as in core-collapse SNe and a lesser amount in gravitational wave. Only a small fraction, $\sim 10^{51}$ erg, is converted to a GRB fireball, which

eventually produces a highly-relativistic bi-polar jet and is responsible for the observed γ rays [63, 64].

As discussed previously, observations of supernovae associated with long GRBs provide strong support for the core-collapse scenario for this class of GRBs. The binary merger scenario of short GRBs has not been confirmed, but remains the most popular model.

A. GRB fireball model

The GRB fireball is produced when large amount of energy is released within a short time scale. The isotropic-equivalent energy is $E_{iso} = (4\pi/\Omega_j)E_j$, where Ω_j is the jet solid angle. The average solid angle $\langle\Omega_j\rangle/4\pi \sim 1/500$ or the jet half-opening angle $\langle\theta_j\rangle \sim 1/10$ [12, 96, 97]. The luminosity of the outflowing material is $L_{iso} \sim E_{iso}/t$, where t is the typical duration of a long GRB. The temperature of the outflowing material at the base of the jet, with an inner radius of an accretion disc $r_0 \sim 10^7$ cm, is $kT = (L_{iso}/4\pi r_0^2 ca) \sim \text{few MeV}$. Here $a = 7.6 \times 10^{-15}$ ergs cm $^{-3}$ K $^{-4}$ is the radiation density constant. The fireball contains gamma rays, electron-positron pairs and relatively fewer baryons (mostly protons). Due to the radiation pressure, the optically thick hot plasma expands and overcome the gravitational pressure and forms the relativistic jet [99].

An initially thermal energy dominated GRB jet becomes kinetic energy dominated when the baryons carry the bulk of the initial fireball energy at a saturation radius $> r_0$ [98]. The bulk Lorentz factor of the jet initially increases as $\Gamma(r) \sim r/r_0$ and becomes constant at a value $\Gamma \sim \eta \sim 10^2\text{--}10^3$, where $\eta \sim L_{iso}/\dot{M}c^2$ is defined as the ratio between the total energy to mass flow and is called the baryon loading of the fireball. The radius at which the fireball attains this coasting Lorentz factor is $\sim r_0\eta$ [100, 101].

B. Prompt keV–MeV emission

The prompt γ -rays from a GRB are thought to be emitted when a significant fraction of the fireball kinetic energy is converted back to radiation energy. The internal shocks model is currently the most popular model for prompt γ -ray emission [102]. Collisions between shells of plasma or fireball produce shocks and a fraction of the bulk kinetic energy is converted into random particle energy which is then radiated, via synchrotron mechanism e.g., as the observed non-thermal γ rays. Given a timescale t_v from observations of highly variable prompt γ -ray emission, internal shock collisions take place, due to a difference in Lorentz factor $\Delta\Gamma \sim \Gamma$ between the shells, at a radius $r_i \sim \Gamma^2 ct_v \sim 3 \times 10^{13}(\Gamma/316)^2(t_v/0.01 \text{ s})$ cm. This is typically much larger than the photospheric radius of a baryon-dominated GRB jet, given by $r_{ph} \sim \sigma_T L_{iso}/(4\pi\Gamma^3 m_p c^3) \sim 4 \times 10^{12}(L_{iso}/10^{52} \text{ erg s}^{-1})(\Gamma/316)^3$ cm (see, however, [103]

for different scaling of the photosphere). The observed pulse structure can be produced in colliding shells model [104, 105]. Note that the variability time scale can be as small as ~ 1 ms, corresponding to the size scale of the jet base r_0 .

The internal shocks are semi-relativistic, with Lorentz factor $\Gamma_{sh} \sim \text{few}$. A fraction of the shock energy is thought to amplify magnetic field, via some kind of instabilities, up to an energy that is at some equipartition level ϵ_B with the jet luminosity L_{iso} [106, 107]. Another fraction of the shock energy is thought to accelerate electrons, via a Fermi mechanism, to relativistic energies. In a fast-cooling scenario, where electrons lose most of their energy to the observed radiation, e.g. via synchrotron/Compton mechanism, within the dynamic time scale, the prompt γ -ray luminosity $L_{\gamma,iso}$ can be used to infer L_{iso} (and eventually E_{iso} from the duration of the burst) as $L_{iso} = L_{\gamma,iso}/\epsilon_e$. The magnetic field in the jet frame can also be inferred from the prompt γ -ray observations as $B' = (2\epsilon_B L_{\gamma,iso}/\epsilon_e r_i^2 \Gamma^2 c)^{1/2} \sim 2 \times 10^4(\epsilon_B/\epsilon_e)^{1/2}(L_{\gamma,iso}/10^{51} \text{ erg s}^{-1})^{1/2}(\Gamma/316)^{-3}(t_v/0.01 \text{ s})^{-1}$ Gauss [108]. With a minimum Lorentz factor of the electrons, $\gamma_e \sim m_p/m_e$, characteristic synchrotron radiation peak can explain the observed $\varepsilon_{pk} \sim \text{few hundred keV}$ typical νF_ν peak of the γ -ray spectrum. The power-law part of the observed Band spectra above ε_{pk} can be explained as due to synchrotron radiation from the power-law distributed electron Lorentz factor, $n(\gamma_e) \sim \gamma_e^{-p}$, as $n(\varepsilon) \sim \varepsilon^{-p/2-1}$.

The synchrotron shock model as described above has difficulties to explain the observed γ -ray spectrum below ε_{pk} in a large fraction of the bursts [109–111]. The fast-cooling synchrotron model is expected to produce a spectrum $n(\varepsilon) \sim \varepsilon^{-3/2}$ below ε_{pk} as contrary to ε^{-1} , typical observed value. A harder, $\varepsilon^{-2/3}$, synchrotron spectrum from electrons in random magnetic field is often called the “synchrotron death line” [109] which too has been observed violated in a sizeable fraction of GRBs.

There have been many attempts to solve this Band spectrum crisis within the synchro-Compton mechanism. Explanations include synchrotron self-absorption in the keV range [112], Compton scattering of optical photons to keV energies [113], low-pitch angle scattering or jitter radiation [114, 115], time-dependent acceleration [116] as well as mixing of keV photons with axion-like particles [117]. Photospheric thermal emission, as we describe next, holds promise to explain the hard Band spectrum below ε_{pk} .

C. Photospheric emission

In case of a baryon-loaded GRB fireball, as we discussed before, most of the thermal energy converts to kinetic energy at a radius $r > r_0\eta$. The photospheric radius r_{ph} is also typically much larger than $r_0\eta$. In case the fireball is highly baryon dominated r_{ph} is smaller and could become comparable to $r_0\eta$. A significant fraction

of the thermal energy can be released from the fireball in this case [100]. Moreover dissipation of kinetic energy at or below the photosphere, by shocks or other mechanisms such as neutron-proton decoupling and interactions [101, 118–120], could also enhance thermal radiation for moderately baryon-loaded fireballs as well as explain highly-efficient γ -ray emission from GRBs, which is difficult to explain with internal shocks.

Simple photospheric models should produce thermal emission peaking at ~ 1 MeV, the temperature of the fireball at the base of the jet, which is in the range of observed Band peaks [121, 122]. This leads to a plausible physical explanations for the Amati [123] or Ghirlanda [124] relations between the νF_ν peak energy and the total γ -ray energy [121, 125]. The temperature of the photosphere can be much below ~ 1 MeV in more complicated models, see e.g. [103]. Neutron-proton decoupling, their interactions and resulting radiation from cascade particles at the photosphere or Compton scattering of thermal photons by relativistic electrons in sub-photospheric shocks have also been explored to produce the phenomenological Band spectrum. These processes explain the power-law spectrum above ε_{pk} . The “synchrotron death line” issue [109] below ε_{pk} can be avoided in photospheric models.

Recent modeling of Fermi data from GRB 090902B provides some evidence of photospheric emission being dominant in this burst [126]. In some other Fermi bursts a photospheric component in addition to the Band or Comptonized spectrum seems to improve fits, although thermal emission is not dominant in these bursts [127, 128].

D. Poynting flux dominated GRB model

Fermi observations of GRBs over a broad energy range and non-detection of a strong photospheric component in almost all bursts, and specially after GRB 080916C [22, 129], have renewed interests in magnetic or Poynting-flux dominated GRB jets, . A large dissipation radius, $r \sim 10^{15}$ cm, yet high efficiency inferred from modeling Fermi data can also be explained more naturally with magnetic models. Particles are accelerated in the reconnection region of the magnetic field lines and produce the observed radiation. Magnetic models can be generalized into two categories. In the first category the baryons are completely absent in the jet or dynamically negligible, at least initially [130–132], and in the second category the baryon load is significant but dynamically sub-dominant relative to the magnetic stresses [133–136]. A hybrid model, dubbed ICMART [137] involves an initially Poynting-flux dominated outflow with few baryons that lead to internal shocks when the magnetic energy subsides at a large radius.

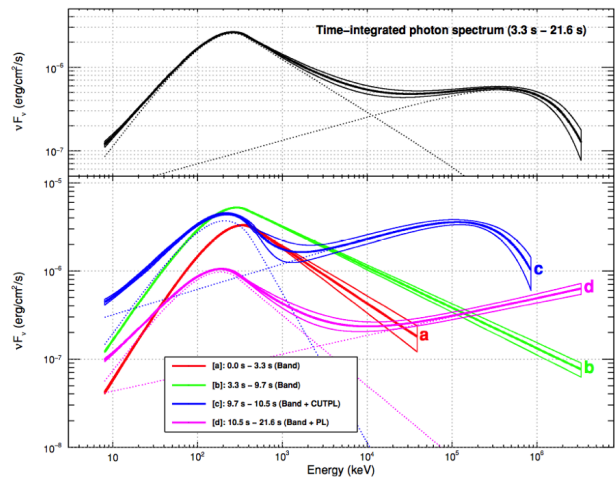


FIG. 8: Prompt emission spectra of GRB 090926A at different time intervals (bottom panel) as well as during the entire prompt phase (top panel). A power-law component in addition to the Band spectrum, as also found in other bright LAT-detected GRBs, is required to fit spectra. A cutoff in the PL component at few GeV has been detected in this GRB and in GRB 110731A [138]. From Abdo et al. [26].

E. GeV emission and plausible interpretations

The origin of $\gtrsim 100$ MeV radiation from GRBs and associated additional spectral component (Figure 8) has been intensely debated in recent years. In the context of the internal shock scenario, Synchrotron-Self-Compton (SSC) scattering of soft target photons by relativistic electrons is the first choice to produce the hard power-law component in a simple one-zone model [24, 139–142]. The observed time delay (Figure 2) between the keV–MeV radiation and $\gtrsim 100$ MeV radiation, however, is longer than the expected delay for the SSC emission, which can be of the order of the variability time scale ($\lesssim 1$ s for long bursts) at best. Compton radiation from late internal shocks, with much longer variability time at GeV than in keV–MeV, can explain delayed LAT onset in some cases [140, 142].

An alternate mechanism to produce $\gtrsim 100$ MeV radiation in the prompt GRB phase is through hadronic emission, either proton-synchrotron radiation and radiation from $\gamma\gamma \rightarrow e^+e^-$ pair cascades [143] (Figure 9) or photohadronic interactions and associated cascade radiation [144, 145] (Figure 10). In the one-zone radiating shells, the hadronic models can account for the delayed detection of the hard power-law component through required proton acceleration and cooling time.

The total energy of the burst, however, needs to be rather large in hadronic models because of a high jet Lorentz factor, $\Gamma \gtrsim 500$, required to avoid $\gamma\gamma$ pair production *in-situ* by $\gtrsim 1$ GeV photons. In particular, to generate the observed 2.44 s delay in LAT for GRB 110731A the comoving frame jet magnetic field needs to be $B' \approx 10^5 (\Gamma/500)^{-1/3} (t_{\text{onset}}/2.44 \text{ s})^{-2/3}$

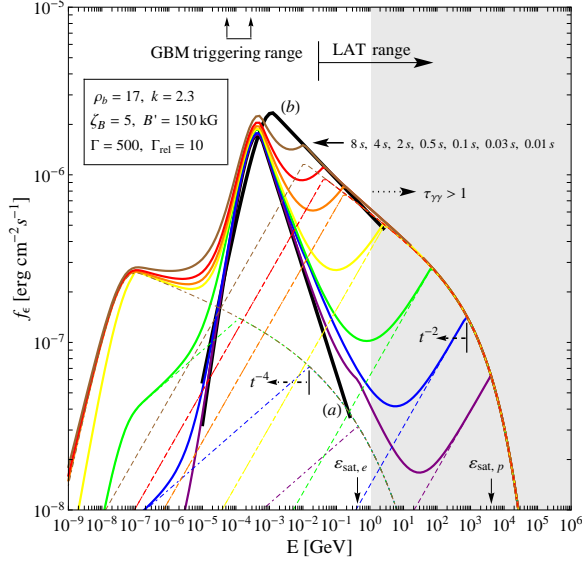


FIG. 9: Proton-synchrotron radiation model for delayed onset of LAT emission in GRB 080916C. The delay is caused by a build-up of proton-synchrotron flux and a shift of cooling frequency from very high energies to the LAT range, with time. GBM radiation is assumed to be dominated by electron-synchrotron radiation. From [143].

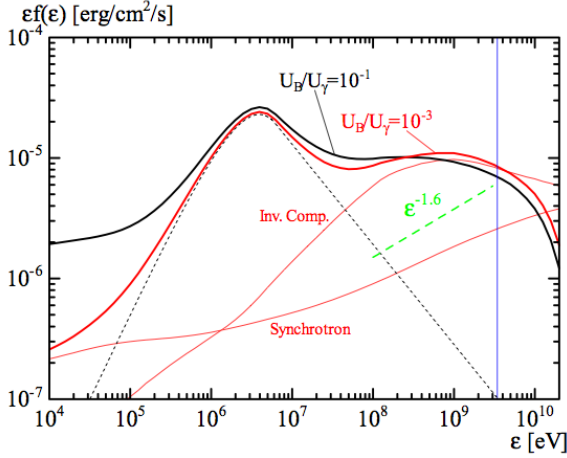


FIG. 10: Photohadronic cascade radiation model for the additional power-law component detected in GRB 090510. Synchrotron radiation from charged pions, muons and e^+e^- contribute to the observed spectra. High-energy neutrinos are also expected in this model. From [144].

$(E_\gamma/100 \text{ MeV})^{-1/3} \text{ G}$, in case of proton-synchrotron model. The corresponding isotropic-equivalent jet luminosity is $L_{\text{jet}} \gtrsim 10^{57} (\Gamma/500)^{16/3} (t_{\text{onset}}/2.44 \text{ s})^{2/3} (E_\gamma/100 \text{ MeV})^{-2/3} \text{ erg s}^{-1}$ [139, 143]. While the hadronic models require a larger total energy than the leptonic models, the energy budget can be brought down for $\Gamma < 500$, see also [146, 147].

A high Γ is not a prerequisite to avoid $\gamma\gamma$ absorption in case of two-zone radiation, in either leptonic or hadronic

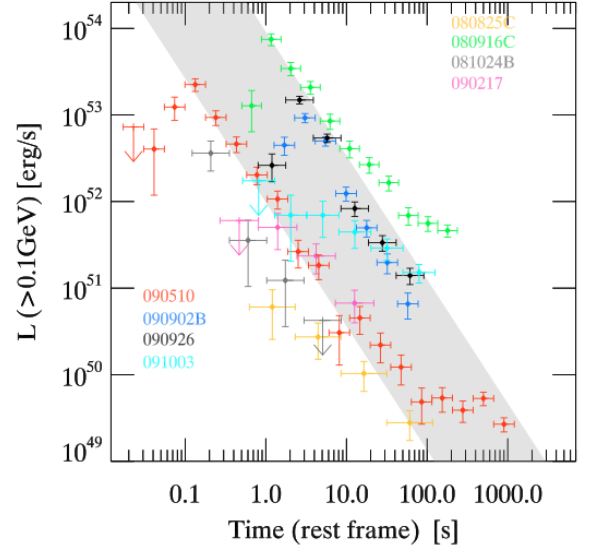


FIG. 11: Light curves of $\gtrsim 100 \text{ MeV}$ radiation from a few LAT-detected GRBs, which show decaying LAT flux as a common feature. The grey band with slope $t^{-10/7}$ is the expected decay behavior for afterglow emission from a radiative blast wave. From [151].

models, where LAT emission comes from late internal shocks [142, 143, 148, 149]. The late internal shocks, however, can not explain temporally extended LAT emission which is apparently non-variable.

The delayed onset, longer duration and smooth temporal decay of the $\gtrsim 100 \text{ MeV}$ flux (Figure 11) led to the development of an early afterglow interpretation of high-energy radiation from the external forward shock [28, 29, 150–152]. The time delay between keV–MeV radiation and $\gtrsim 100 \text{ MeV}$ radiation is explained as the time required for deceleration of the GRB jet with high Γ . The hard power-law component and temporally-extended LAT emission are interpreted as synchrotron radiation from the external shock while keV–MeV emission from the internal shocks in these two-zone emission models. Detailed modeling, however, shows that an extrapolation of the external shock emission at earlier time fails to reproduce all of the $\gtrsim 100 \text{ MeV}$ flux in the prompt phase, requiring a significant contribution from the internal dissipation regions [30, 153–155].

Both in the internal- and external-shock scenario, modeling of high-energy radiation by the leptonic and/or hadronic processes depends crucially on Γ . Currently $\gamma\gamma \rightarrow e^+e^-$ pair-production constraint in internal shocks is the most widely used estimate of a lower limit on Γ [108, 156, 157]. In the case of GRB 090926A and GRB 110731A a cut off in the additional power-law component allowed to estimate Γ rather than its lower limit, assuming that the cut off at GeV energy is due to attenuation of flux by $\gamma\gamma \rightarrow e^+e^-$ pair absorption. Figure 12 shows the estimates of Γ from *Fermi* LAT-detected bright GRBs. There are, however, large (a factor 2–3)

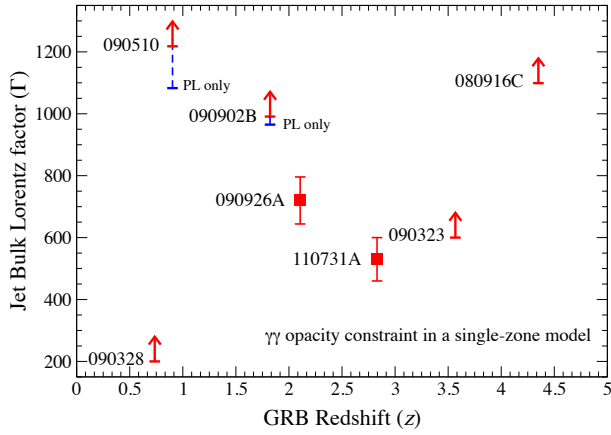


FIG. 12: Bulk Lorentz factors of Fermi-LAT detected GRB jets calculated from $\gamma\gamma \rightarrow e^+e^-$ pair absorption effect of GeV photons assuming that they are produced in the same physical region as the lower, $\lesssim 100$ MeV, photons. The lower limits, Γ_{min} , are calculated in cases where there were no cutoff in the spectra in the GeV range. In the “PL only” lower limits on Γ_{min} were calculated using only the additional power-law components of the spectra. Estimates of Γ rather than Γ_{min} were made when the observed $\gtrsim 1$ GeV cutoff in the spectra were assumed due to $\gamma\gamma \rightarrow e^+e^-$ pair absorption.

uncertainty due to theoretical modeling of target radiation fields and environment [24, 158–160].

F. GRB afterglow

Regardless of the details of the dissipation mechanism of the GRB jet to produce prompt γ -ray emission, the accumulated surrounding material by the jet drives a blast wave and external forward shock [161]. A reverse shock is also expected in the baryon-loaded fireballs. The deceleration takes place with the jet energy comparable to the kinetic energy of the swept-up material in the blast wave, $E_{iso} = (4/3)\pi r_{dec}^3 n_{ext} m_p c^2 \Gamma^2$. The deceleration radius is $r_{dec} \sim 2 \times 10^{17} (E_{iso}/10^{53} \text{ erg})^{1/2} (n_{ext}/1 \text{ cm}^{-3})^{-1/2} (\Gamma/100)^{2/3} \text{ cm}$ for a constant density external medium.

After deceleration, the blast wave evolves in a self-similar fashion with the bulk Lorentz factor decreasing as $\Gamma \sim t^{-3/8}$ for an adiabatic fireball and $\Gamma \sim t^{-3/7}$ for a radiative fireball, both in constant density medium [161, 162]. Particles are expected to be accelerated in the forward shock, which is highly relativistic. Magnetic field also assumed to be generated in the forward shock, which leads to synchrotron radiation by relativistic particles [162, 163]. As the jet continues to be decelerated in the course of sweeping up more and more external matter, the peak of the synchrotron flux shifts from high-frequency to low-frequency bands. Smooth decay of the flux across different energy bands is a characteristic feature of the afterglow synchrotron model [164], whose pre-

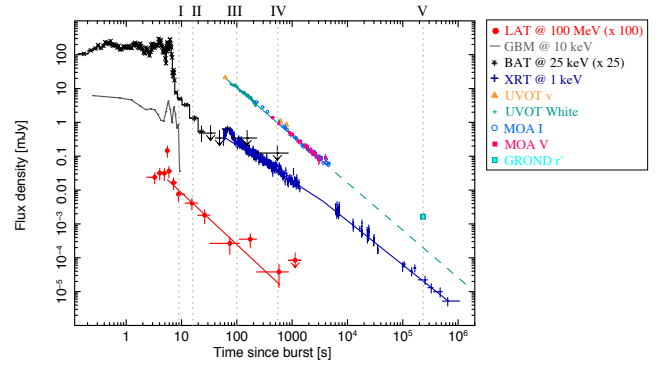


FIG. 13: Multiwavelength light curves of GRB 110731A from *Fermi* GBM and LAT; *Swift* BAT, XRT and UVOT; and ground-based optical telescopes. Smooth decay of the fluxes across the wavelengths after ~ 6 s suggests their origin, including LAT emission, as from a decelerating blast wave in stellar wind environment. From [138].

dicted detection allowed the first measurements of host galaxies and redshift distances [4, 5].

Broadband X-ray to radio emission from GRBs has been quite successfully described by synchrotron radiation from a decelerating blast wave with or without variation of the straightforward models. Prompt optical emission [164], at the time the deceleration has been detected, with robotic ground-based telescopes such as ROTSE and others. The external shock interpretation of the late afterglow has proven robust overall, although some detailed features such as the X-ray steep decays followed by flat plateaus and occasional large flares are not well-understood yet.

As discussed in Section III E, temporally extended $\gtrsim 100$ MeV emission detected by Fermi-LAT from many GRBs well after the prompt keV–MeV emission has been advocated as afterglow emission by a number of authors [28, 29, 150–152]. To test an early afterglow interpretation of the LAT data from GRBs one needs to confront models with simultaneous multiwavelength data sets. Most recently, modeling of multiwavelength light curves (Figure 13) and broadband Spectral Energy Distribution (SED) from GRB 110731A (Figure 14) strongly indicate that [138] (i) LAT extended emission as early as $T_0 + 8.3$ s, from broadband SED, is compatible with afterglow synchrotron emission in other bands. (ii) A wind afterglow model [165–167] is favored over an ISM model, from the behavior of the light curves and SEDs. Detailed modeling of GRB 110731A data also resulted in $\Gamma \sim 500$ just before deceleration of the blast wave [138]. An internal shock contribution to LAT data before $T_0 + 8.3$ s can not be ruled out, however, and requires detailed investigation with future Swift-Fermi bursts.

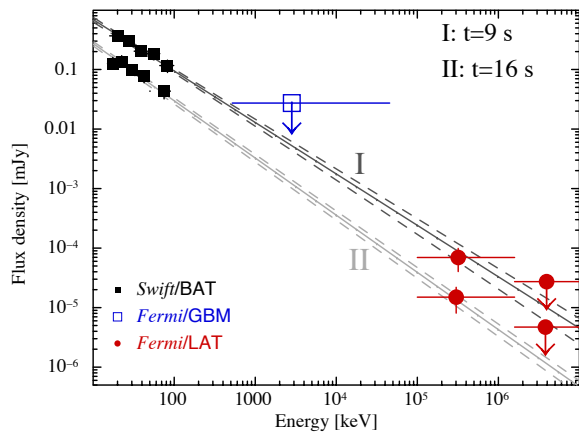


FIG. 14: Broadband spectra of GRB 110731A at two time intervals after the trigger. Single power laws fitting the spectra, together with flux decay behavior in Fig. 13 imply that LAT emission is afterglow. From [138].

G. High-energy neutrinos from GRBs

Neutrinos with energies $\gtrsim 100$ TeV are expected from photohadronic ($p\gamma$) interactions of relativistic protons accelerated in the fireball internal or external shocks. In the case of internal shocks, the interaction is expected to take place between MeV photons produced by radiation from accelerated electrons and protons which are co-accelerated in the same shocks [168–171]. Neutrinos are expected to be produced more efficiently at an energy $\varepsilon_\nu \gtrsim 100(\varepsilon_{\gamma,pk}/100 \text{ keV})^{-1}(\Gamma/316)^2$ TeV. Neutrino production in internal shocks is expected to suppress at an energy $\varepsilon_\nu \gtrsim 1$ PeV due to synchrotron and adiabatic losses of the high-energy pions and muon [169, 172, 173]. In the case of external shocks, optical/UV photons predominantly take part in $p\gamma$ interactions to produce $\gtrsim 1$ EeV neutrinos [174–176].

The most intense neutrino emission at $\lesssim 10$ TeV energies from GRBs or collapsars might be due to p, γ and pp interactions occurring *inside* the stellar envelope while the jet is still burrowing its way out of the star [177, 178] and before it successfully break through the stellar envelope to produce a GRB or choke inside. Figure 15 shows different neutrino flux models [179] from a nearby GRB 030329 at $z = 0.17$ which was also connected with a supernova.

The IceCube Collaboration has recently constrained high-energy neutrino emission from the internal shocks by stacking electromagnetic data from GRBs [180–182]. This constraint, in the ~ 1 –20 PeV energy range, calculated from 40 and 59 string data severely excludes efficient neutrino production in the internal shocks. This could be due to the high bulk Lorentz factor, $\gtrsim 500$, of the GRB jet which reduces photopion production efficiency, e.g. [147, 183], or due to inefficient acceleration of protons in the internal shocks. To accommodate IceCube non-detection, revisions to the neutrino flux from

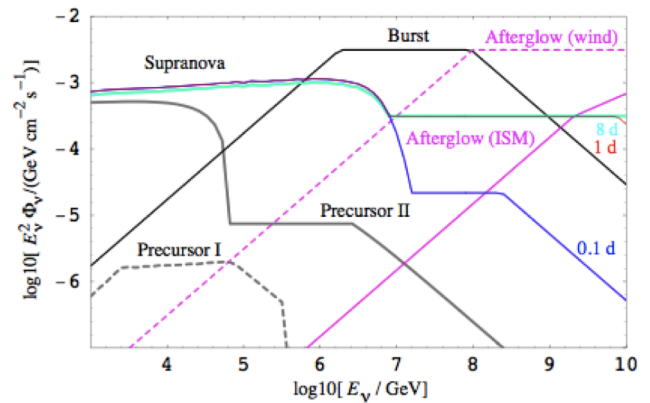


FIG. 15: Predicted neutrino fluxes from a relatively nearby GRB 030329 at a redshift $z = 0.17$. An accompanying supernova was detected from this long GRB as well. From [179].

internal shocks have also been proposed [184, 185]. New calculations in the models alternate to internal shocks are being done as well, e.g. [186]. Data from the full IceCube detector will either constrain the neutrino production efficiency in the internal shocks or rule out these models. Note that TeV neutrinos from the buried GRB jet [177, 178] and EeV neutrinos from the afterglow [174–176] remain viable.

H. Gravitational waves from GRB

Binary mergers of NS-NS and/or NS-BH, the most popular model for short GRBs, are the strongest candidate sources of gravitational waves (GWs) with a total energy reaching $\sim 10^{54}$ ergs [187, 188]. The luminosity of GW from long GRBs, originating from core-collapse of massive stars, is highly model-dependent [189]. Recent numerical calculations of GW emission from long GRBs range from pessimistic [190] to modest [191] predictions. The expected detection rates of GW from compact binary mergers in coincidences with short GRBs have been estimated to be several per year [192] for the advanced LIGO and VIRGO. Coordinated detection of GW with electromagnetic signal helps to reduce background significantly, if short GRBs are the sources. Combining sub-threshold signal from electromagnetic, neutrino and GW observatories can also lead to significant detection [193].

IV. FUTURE GRB OBSERVATIONS

Both Swift and Fermi are healthy and adequately-funded by NASA and foreign partners. Neither has lifetime limits from expendable propulsion gasses or cryogenics, and both have orbital lifetimes beyond 2025. They are joined by INTEGRAL (e.g., Mereghetti et al. 2003 [194]) and MAXI [195], which also detect GRBs and the InterPlanetary Network of GRB detectors [196] that lo-

calize events by triangulating their arrival times.

There are several future missions with GRB capabilities that are being developed or proposed. They include:

1. SVOM – A Chinese-French mission to detect GRBs and perform rapid optical and X-ray follow-up [197].
2. UFFO – A Korean payload flying on the Russian Lomonosov mission [198]. The payload includes a wide-field hard X-ray burst detector and a rapidly-orienting optical telescope. The pathfinder version of the mission will fly in 2012.
3. Lobster – A wide-field focusing X-ray instrument operating in the 0.4–4 keV band. There are several versions that have been proposed including a UK instrument on the International Space Station [199], a NASA Explorer mission including an afterglow IR telescope [200], and an Explorer Mission of Opportunity on the International Space Station [201].
4. LOFT – A large-area X-ray timing mission selected for a Phase A study for ESA’s M2 opportunity [202].
5. ASTROSAT – An Indian mission with hard X-ray imager, scanning sky monitoring, X-ray and UV telescopes [203].

Fermi LAT detection of > 10 GeV photons indicate that the prospects for detection of VHE radiation from GRBs by ground-based telescopes are promising. Highly sensitive Imaging Atmospheric Cherenkov Telescopes (IACTs) such as MAGIC, VERITAS and HESS with a threshold energy as low as 25 GeV (special GRB mode for MAGIC) are currently slewing to the GRB directions. Water Cherenkov detector HAWC is also under construction. Simultaneous observations by Fermi LAT and Cherenkov telescopes in the overlapping energy range will be extremely helpful to understand the nature of high-energy radiation from GRBs. Such observations can also pose strong constraints on both the leptonic and hadronic models, especially independent handles on the magnetic field strength are possible. Long-sought SSC radiation from the external forward shock or hadronic radiation in the prompt phase can also be searched for and/or constrained. Detection of very-high energy radiation from GRBs can be modeled to estimate the total explosion energy, which has implications for Gravitational Wave detection by LIGO/VIRGO.

There is a great opportunity for new science coming from future observations coordinated with GRBs of gravitational waves, neutrinos and across the electromagnetic spectrum. There are major new facilities coming

on line and planned such as LIGO/VIRGO, IceCube, PanSTARRS, LSST and the 30m telescopes.

V. CONCLUSIONS

We are in an era of rapid progress in understanding GRBs. Swift, Fermi, INTEGRAL, MAXI, and IPN are all detecting GRBs. A vibrant community of observers is following up the GRB detections with new and capable instruments across the electromagnetic spectrum. Key findings from the past several years has included the following:

1. X-ray afterglow features, steep and shallow decays, flares,
2. afterglows and accurate localizations of short bursts supporting a possible merger origin,
3. confirmation of long GRB-Supernova connection,
4. detection of high-redshift, $z > 5$, GRBs,
5. delayed onset of GeV emission,
6. high bulk Lorentz factor of the jet.

With all this progress, there are many objectives that we hope to accomplish in the next 10 years. These include:

1. confirmation of short burst origin,
2. jet opening angle and measurements of lightcurve breaks
3. metallicity dependence
4. relation to star formation history
5. nature and interpretation of high energy spectral components.

We look forward to many years more of GRB discovery.

VI. ACKNOWLEDGEMENTS

We thanks John Cannizzo and Charles Dermer for valuable consultation and comments on this paper. All data from the Swift and Fermi observatories are publicly available through NASA’s High Energy Astrophysics Science Archive Research Center (HEASARC) at <http://heasarc.gsfc.nasa.gov/>. Work of S.R. was supported by NASA Fermi Guest Investigator program and was performed at the Naval Research Lab while under contract.

- [3] C. Kouveliotou, et al., *Astrophys. J.* 413, 101 (1993)
- [4] E. Costa, et al., *Nature* 387, 783 (1997)
- [5] J. van Paradijs, et al., *Nature* 386, 686 (1997)
- [6] F. A. Harrison, et al., *Astrophys. J. Lett.* 523, L121 (1999)
- [7] N. Gehrels, et al., *Astrophys. J.* 611, 1005 (2004)
- [8] S. D. Barthelmy, et al., *Space Sci. Rev.* 120, 143 (2005)
- [9] D. N. Burrows, et al., *Space Sci. Rev.* 120, 165 (2005)
- [10] P. W. A. Roming, et al., *Space Sci. Rev.* 120, 95 (2005)
- [11] P. T. O'Brien et al., *Astrophys. J.* 647, 1213 (2006)
- [12] N. Gehrels, et al., *Annual Rev. Astron. Astrophys.* 47, 567 (2009)
- [13] J. A. Nousek, et al., *Astrophys. J.* 642, 389 (2006)
- [14] B. Zhang, et al., *Astrophys. J.* 642, 354 (2006)
- [15] D. N. Burrows et al., *Science*, 309, 1833 (2005)
- [16] A. S. Fruchter, et al., *Nature* 441, 463 (2006)
- [17] A. I. MacFayden & S. E. Woosley, *Astrophys. J.* 524, 262 (1999)
- [18] V. V. Usov, *Nature* 357, 472 (1992)
- [19] A. M. Soderberg, et al., *Nature* 442, 1014 (2006)
- [20] C. Meegan, et al., *Astrophys. J.* 702, 791 (2009)
- [21] W. B. Atwood, et al., *Astrophys. J.* 697, 1071 (2009)
- [22] A. A. Abdo, et al., *Science*, 323, 1688 (2009)
- [23] A. A. Abdo, et al., *Nature*, 462, 331 (2009)
- [24] M. Ackermann, et al., *Astrophys. J.* 716, 1178 (2010)
- [25] A. A. Abdo, et al., *Astrophys. J. Lett.* 706, L138 (2009)
- [26] M. Ackermann, et al., *Astrophys. J.* 729, 114 (2011)
- [27] A. A. Abdo, et al., *Astrophys. J.* 712, 558 (2010)
- [28] M. De Pasquale, et al., *Astrophys. J. Lett.* 709, L146 (2010)
- [29] S. Razzaque, *Astrophys. J. Lett.* 724, L109 (2010)
- [30] H.-N. He, et al., *Astrophys. J.* 733, 22 (2011)
- [31] N. Kawai, et al., *Nature*, 440, 184 (2006)
- [32] J. Greiner, et al., *Astrophys. J.* 693, 1610 (2009)
- [33] N. R. Tanvir, et al., *Nature* 461, 1254 (2009)
- [34] R. Salvaterra, et al., *Nature* 461, 1258 (2009)
- [35] A. Cucchiara, et al., *Astrophys. J.* 736, 7 (2011)
- [36] S. Savaglio, *New J. Phys.* 8, 195 (2006)
- [37] E. M. Levesques, et al., *Astrophys. J.* 725, 1337 (2010)
- [38] M. D. Kistler, et al., *Astrophys. J.* 705, L104 (2009)
- [39] B. E. Robertson & R. S. Ellis, *Astrophys. J.* 744, 95 (2012)
- [40] A. M. Hopkins & J. F. Beacom, *Astrophys. J.* 651, 142 (2006)
- [41] K. Ota, et al., *Astrophys. J.* 677, 12 (2008)
- [42] R. J. Bouwens, et al., *Astrophys. J.* 686, 230 (2008)
- [43] P. Madau, et al., *Astrophys. J.* 514, 648 (1999)
- [44] S. Campana, et al., *Nature* 476, 421 (2006)
- [45] E. Pian, et al., *Nature*, 442, 1011 (2006)
- [46] P. A. Mazzali, et al., *Nature*, 442, 1018 (2006)
- [47] A. M. Soderberg, et al., *Nature*, 453, 469 (2008)
- [48] E. Liang, B. Zhang and Z. G. Dai, *Astrophys. J.* **662**, 1111 (2007)
- [49] N. Gehrels, et al., *Nature*, 437, 851 (2005)
- [50] J. S. Bloom, et al., *Astrophys. J.* 638, 354 (2006)
- [51] S. D. Barthelmy, et al., *Nature*, 438, 994 (2005)
- [52] E. Berger, et al., *Nature*, 438, 988 (2005)
- [53] D. B. Fox, et al., *Nature*, 437, 845 (2005)
- [54] J. Hjorth, et al., *Nature*, 437, 859 (2005)
- [55] J. S. Villaseñor, et al., *Nature*, 437, 855 (2005)
- [56] C. N. Leibler, & E. Berger, *Astrophys. J.* 725, 1202 (2010)
- [57] W. Fong, E. Berger, D. B. Fox, *Astrophys. J.* 708, 9 (2010)
- [58] E. Nakar, *Phys. Reports*, 442, 166 (2007)
- [59] D. Eichler, et al., *Nature*, 340, 126 (1989)
- [60] B. Paczynski, *Acta Astronomica*, 41, 257 (1991)
- [61] B. Zhang, B. -B. Zhang, F. J. Virgili, E. -W. Liang, D. A. Kann, X. -F. Wu, D. Proga and H. -J. Lv *et al.*, *Astrophys. J.* **703**, 1696 (2009)
- [62] O. Bromberg, E. Nakar, T. Piran and R. 'e. Sari, arXiv:1210.0068 [astro-ph.HE].
- [63] N. Gehrels & P. Mészáros, *Science*, 337, 932 (2012)
- [64] P. Mészáros & N. Gehrels, *Research in Astronomy and Astrophysics*, 12, 1139 (2012)
- [65] D. N Burrows, et al., *Astrophys. J.* 653, 468 (2006)
- [66] W. Fong, et al., *Astrophys. J.* 756, 189 (2012)
- [67] J. P. Norris & J. T. Bonnell, *Astrophys. J.* 643, 266 (2006)
- [68] N. Gehrels, et al., *Nature*, 444, 1044 (2006)
- [69] L. S. Finn, et al., *Phys. Rev. D*, 60, 121101 (1999)
- [70] N. Gehrels & J. K. Cannizzo, *Philosophical Trans. A*, accepted (2012)
- [71] S. T. Holland, et al., *GCN* 4034 (2005)
- [72] C. B. Markwardt, et al., *GCN* 4037 (2005)
- [73] J. P. U. Fynbo, et al., *Nature*, 444, 1047 (2006)
- [74] A. Gal-Yam, et al., *Nature*, 444, 1053 (2006)
- [75] M. della Valle, et al., *Nature*, 444, 1050 (2006)
- [76] S. B. Cenko, et al., *A. J.* 140, 224 (2010)
- [77] P. Chandra, P. et al., *Astrophys. J.* 683, 924 (2008)
- [78] K. Onda, et al., *P. A. S. J.* 62, 547 (2010)
- [79] M. M. Kasliwal, et al., *Astrophys. J.* 678, 1127 (2008)
- [80] J. J. in't Zand, et al., *A. & A.*, 357, 520 (2000)
- [81] J. A. Orosz, et al., *Astrophys. J.*, 555, 489 (2001)
- [82] Y. Tanaka & N. Shibazaki, *Annual Rev. Astron. Astrophys.* 34, 607 (1996)
- [83] R. A. Remillard & J. E. McClintock, *Annual Rev. Astron. Astrophys.* 44, 49 (2006)
- [84] J. K. Cannizzo, et al., *Astrophys. J.* 454, 880 (1995)
- [85] J. K. Cannizzo, *Astrophys. J.* 494, 366 (1998)
- [86] S. Nayakshin, et al., *Astrophys. J.* 535, 833 (2000)
- [87] J. C. McKinney & R. D. Blandford, *M.N.R.A.S.*, 394, L126 (2009)
- [88] N. Rea, et al., *Astrophys. J. Lett.* 729, L21 (2011)
- [89] V. Simon, et al., *M.N.R.A.S.*, 422, 981 (2012)
- [90] G. Dubus, et al., *A. & A.*, 373, 251 (2001)
- [91] J. E. McClintock & R. A. Remillard, *Astrophys. J.*, 308, 110 (1986)
- [92] C. C. Thöne, et al., *Nature*, 480, 72 (2011)
- [93] S. Campana, et al., *Nature*, 480, 69 (2011)
- [94] R. Narayan, B. Paczynski and T. Piran, *Astrophys. J.* **395**, L83 (1992)
- [95] M. Vietri and L. Stella, *Astrophys. J. Lett.* **527**, L43 (1999)
- [96] D. A. Frail, S. R. Kulkarni, R. Sari, S. G. Djorgovski, J. S. Bloom, T. J. Galama, D. E. Reichart and E. Berger *et al.*, *Astrophys. J.* **562**, L55 (2001)
- [97] S. B. Cenko, D. A. Frail, F. A. Harrison, S. R. Kulkarni, E. Nakar, P. Chandra, N. R. Butler and D. B. Fox *et al.*, *Astrophys. J.* **711**, 641 (2010)
- [98] A. Shemi and T. Piran, *Astrophys. J.* **365**, L55 (1990).
- [99] P. Mészáros, P. Laguna and M. J. Rees, *Astrophys. J.* **415**, 181 (1993)
- [100] P. Mészáros and M. J. Rees, *Astrophys. J.* **530**, 292 (2000) [astro-ph/9908126].
- [101] E. M. Rossi, A. M. Beloborodov and M. J. Rees, *Mon. Not. Roy. Astron. Soc.* **369**, 1797 (2006)
- [102] M. J. Rees and P. Mészáros, *Astrophys. J.* **430**, L93

- (1994)
- [103] P. Veres and P. Mészáros, *Astrophys. J.* **755**, 12 (2012)
 - [104] C. D. Dermer, *Astrophys. J.* **614**, 284 (2004)
 - [105] S. Kobayashi, T. Piran and R. 'e. Sari, *Astrophys. J.* **490**, 92 (1997)
 - [106] M. V. Medvedev and A. Loeb, *Astrophys. J.* **526**, 697 (1999)
 - [107] T. Inoue, K. Asano and K. Ioka, *Astrophys. J.* **734**, 77 (2011)
 - [108] S. Razzaque, P. Mészáros and B. Zhang, *Astrophys. J.* **613**, 1072 (2004)
 - [109] R. D. Preece, M. S. Briggs, R. S. Mallozzi, G. N. Pendleton, W. S. Paciesas and D. L. Band, *Astrophys. J. Lett.* **506**, L23 (1998)
 - [110] Y. Kaneko, R. D. Preece, M. S. Briggs, W. S. Paciesas, C. A. Meegan and D. L. Band, *Astrophys. J. Suppl.* **166**, 298 (2006)
 - [111] A. Goldstein, J. M. Burgess, R. D. Preece, M. S. Briggs, S. Guiriec, A. J. van der Horst, V. Connaughton and C. A. Wilson-Hodge *et al.*, *Astrophys. J. Suppl.* **199**, 19 (2012)
 - [112] J. Granot, T. Piran, and R. Sari, *Astrophys. J. Lett.* **534**, L163 (2000)
 - [113] A. Panaitescu and P. Mészáros, *Astrophys. J.* **544**, L17 (2000)
 - [114] M. V. Medvedev, *Astrophys. J.* **540**, 704 (2000)
 - [115] M. V. Medvedev, *Astrophys. J.* **637**, 869 (2006)
 - [116] N. M. Lloyd-Ronning and V. Petrosian, *Astrophys. J.* **565**, 182 (2002)
 - [117] O. Mena, S. Razzaque and F. Villaescusa-Navarro, *JCAP* **1102**, 030 (2011)
 - [118] E. V. Derishev, V. V. Kocharovsky & V. V. Kocharovsky *Astrophys. J.* **521**, 640 (1999)
 - [119] S. Razzaque and P. Mészáros, *Astrophys. J.* **650**, 998 (2006)
 - [120] A. M. Beloborodov, *MNRAS* **407**, 1033 (2010)
 - [121] M. J. Rees and P. Mészáros, *Astrophys. J.* **628**, 847 (2005)
 - [122] A. Pe'er, P. Mészáros and M. J. Rees, *Astrophys. J.* **642**, 995 (2006)
 - [123] L. Amati, F. Frontera, M. Tavani, J. J. M. in 't Zand, A. Antonelli, E. Costa, M. Feroci and C. Guidorzi *et al.*, *Astron. Astrophys.* **390**, 81 (2002)
 - [124] G. Ghirlanda, G. Ghisellini and D. Lazzati, *Astrophys. J.* **616**, 331 (2004)
 - [125] C. Thompson, P. Mészáros and M. J. Rees, *Astrophys. J.* **666**, 1012 (2007)
 - [126] A. Pe'er, B. -B. Zhang, F. Ryde, S. McGlynn, B. Zhang, R. D. Preece and C. Kouveliotou, *MNRAS* **420**, 468 (2012)
 - [127] S. Guiriec, M. S. Briggs, V. Connaughton, E. Kara, F. Daigne, C. Kouveliotou, A. J. van der Horst and W. Paciesas *et al.*, *Astrophys. J.* **725**, 225 (2010)
 - [128] S. Guiriec, V. Connaughton, M. S. Briggs, M. Burgess, F. Ryde, F. Daigne, P. Mészáros and A. Goldstein *et al.*, *Astron. J.* **727**, L33 (2011)
 - [129] B. Zhang and A. Pe'er, *Astrophys. J.* **700**, L65 (2009)
 - [130] V. V. Usov, *M.N.R.A.S* **267**, 1035 (1994)
 - [131] P. Mészáros and M. J. Rees, *Astrophys. J. Lett.* **482**, L29 (1997)
 - [132] M. Lyutikov and R. D. Blandford, *astro-ph/0312347*.
 - [133] C. Thompson, *Mon. Not. Roy. Astron. Soc.* **270**, 480 (1994).
 - [134] G. Drenkhahn, *Astron. Astrophys.* **387**, 714 (2002)
 - [135] G. Drenkhahn and H. C. Spruit, *Astron. Astrophys.* **391**, 1141 (2002)
 - [136] C. Thompson, *Astrophys. J.* **651**, 333 (2006)
 - [137] B. Zhang and H. Yan, *Astrophys. J.* **726**, 90 (2011)
 - [138] M. Ackermann, *et al.*, *Astrophys. J.* in press [arXiv:1212.0973](https://arxiv.org/abs/1212.0973) [astro-ph.HE]
 - [139] X. -Y. Wang, Z. Li, Z. -G. Dai and P. Mészáros, *Astrophys. J.* **698**, L98 (2009)
 - [140] Z. Bosnjak, F. Daigne and G. Dubus, *Astron Astrophys.* **498**, 677 (2009)
 - [141] K. Toma, X. -F. Wu and P. Mészáros, *Astrophys. J.* **707**, 1404 (2009)
 - [142] K. Toma, X. -F. Wu and P. Mészáros, *MNRAS* **415**, 1663 (2011)
 - [143] S. Razzaque, C. D. Dermer and J. D. Finke, *Open Astron. J.* **3**, 150 (2010)
 - [144] K. Asano, S. Guiriec and P. Mészáros, *Astrophys. J.* **705**, L191 (2009)
 - [145] K. Murase, K. Asano, T. Terasawa and P. Mészáros, *Astrophys. J.* **746**, 164 (2012)
 - [146] K. Asano, S. Inoue and P. Mészáros, *Astrophys. J.* **725**, L121 (2010)
 - [147] P. Crumley and P. Kumar, *MNRAS* in press, [arXiv:1210.7802](https://arxiv.org/abs/1210.7802) [astro-ph.HE].
 - [148] Z. Li, *Astrophys. J.* **709**, 525 (2010)
 - [149] Y. -C. Zou, Y. -Z. Fan and T. Piran, *Astrophys. J. Lett.* **726**, L2 (2011) [arXiv:1008.2253](https://arxiv.org/abs/1008.2253) [astro-ph.HE].
 - [150] P. Kumar and R. B. Duran, *Mon. Not. Roy. Astron. Soc.* **409**, 226 (2010)
 - [151] G. Ghisellini, G. Ghirlanda, L. Nava & Celotti, *A. MNRAS* **403**, 926 (2010)
 - [152] A. Corsi, D. Guetta and L. Piro, *Astrophys. J.* **720**, 1008 (2010)
 - [153] B. -B. Zhang, B. Zhang, E. -W. Liang, Y. -Z. Fan, X. -F. Wu, A. Pe'er, A. Maxham and H. Gao *et al.*, *Astrophys. J.* **730**, 141 (2011)
 - [154] R. -Y. Liu and X. -Y. Wang, *Astrophys. J.* **730**, 1 (2011)
 - [155] A. Maxham, B.-B Zhang and B. Zhang, *MNRAS*, **415**, 77 (2011)
 - [156] J. H. Krolik & E. A. Pier, *Astrophys. J.* **373**, 277 (1991)
 - [157] Y. Lithwick and R. Sari, *Astrophys. J.* **555**, 540 (2001)
 - [158] M. G. Baring & A. K. Harding, *Astrophys. J.* **491**, 663 (1997)
 - [159] J. Granot, J. Cohen-Tanugi & E. do Couto e Silva, *Astrophys. J.* **677**, 92 (2008)
 - [160] R. Hascoët, F. Daigne, R. Mochkovitch & V. Vennin, *MNRAS* **421**, 525 (2012)
 - [161] R. D. Blandford & C. F. McKee, *Physics of Fluids*, **19**, 1130 (1976)
 - [162] R. Sari, T. Piran & R. Narayan, *Astrophys. J. Lett.* **497**, L17 (1998)
 - [163] P. Mészáros and M. J. Rees, *Astrophys. J.* **476**, 232 (1997)
 - [164] R. A. M. J. Wijers, M. J. Rees and P. Mészáros, *Mon. Not. Roy. Astron. Soc.* **288**, L51 (1997)
 - [165] R. A. Chevalier & Z.-Y. Li, *Astrophys. J.* **536**, 195 (2000)
 - [166] A. Panaitescu and P. Kumar, *Astrophys. J.* **543**, 66 (2000)
 - [167] J. Granot & R. Sari, *Astrophys. J.* **568**, 820 (2002)
 - [168] E. Waxman and J. N. Bahcall, *Phys. Rev. Lett.* **78**, 2292 (1997)
 - [169] J. P. Rachen and P. Mészáros, *Phys. Rev. D* **58**, 123005 (1998)

- [170] C. D. Dermer and A. Atoyan, Phys. Rev. Lett. **91**, 071102 (2003)
- [171] D. Guetta, D. Hooper, J. Alvarez-Muniz, F. Halzen and E. Reuveni, Astropart. Phys. **20**, 429 (2004)
- [172] T. Kashti and E. Waxman, Phys. Rev. Lett. **95**, 181101 (2005)
- [173] P. Lipari, M. Lusignoli and D. Meloni, Phys. Rev. D **75**, 123005 (2007)
- [174] M. Vietri, Phys. Rev. Lett. **80**, 3690 (1998)
- [175] E. Waxman and J. N. Bahcall, Astrophys. J. **541**, 707 (2000)
- [176] Z. G. Dai & T. Lu 2001, Astrophys. J. **551**, 249 (2001)
- [177] P. Mészáros and E. Waxman, Phys. Rev. Lett. **87**, 171102 (2001)
- [178] S. Razzaque, P. Mészáros and E. Waxman, Phys. Rev. D **68**, 083001 (2003)
- [179] S. Razzaque, P. Mészáros and E. Waxman, Phys. Rev. D **69**, 023001 (2004)
- [180] R. Abbasi *et al.* [IceCube Collaboration], Phys. Rev. Lett. **106**, 141101 (2011)
- [181] M. Ahlers, M. C. Gonzalez-Garcia and F. Halzen, Astropart. Phys. **35**, 87 (2011)
- [182] R. Abbasi *et al.* [IceCube Collaboration], Nature **484**, 351 (2012)
- [183] S. Razzaque, C. D. Dermer, J. D. Finke and A. Atoyan, AIP Conf. Proc. **1133**, 328 (2009)
- [184] S. Hummer, P. Baerwald and W. Winter, Phys. Rev. Lett. **108**, 231101 (2012) [arXiv:1112.1076 [astro-ph.HE]]
- [185] H. -N. He, R. -Y. Liu, X. -Y. Wang, S. Nagataki, K. Murase and Z. -G. Dai, Astrophys. J. **752**, 29 (2012)
- [186] B. Zhang and P. Kumar, arXiv:1210.0647 [astro-ph.HE].
- [187] C. S. Kochanek and T. Piran, Astrophys. J. **417**, L17 (1993)
- [188] M. Ruffert and H. T. Janka, Astron. Astrophys. **344**, 573 (1999)
- [189] C. L. Fryer, S. E. Woosley and A. Heger, Astrophys. J. **550**, 372 (2001)
- [190] C. D. Ott, C. Reisswig, E. Schnetter, E. O'Connor, U. Sperhake, F. Löffler, P. Diener and E. Abdikamalov *et al.*, Phys. Rev. Lett. **106**, 161103 (2011)
- [191] K. Kiuchi, M. Shibata, P. J. Montero and J. A. Font, Phys. Rev. Lett. **106**, 251102 (2011)
- [192] J. Abadie *et al.* [LIGO Scientific and Virgo Collaborations], Class. Quant. Grav. **27**, 173001 (2010)
- [193] M. W. E. Smith, D. B. Fox, D. F. Cowen, P. Meszaros, G. Tesic, J. Fixelle, I. Bartos and P. Sommers *et al.*, arXiv:1211.5602 [astro-ph.HE].
- [194] S. Mereghetti, *et al.*, A & A **411**, 291 (2003)
- [195] M. Serino, *et al.*, in 4th International MAXI Workshop, <http://maxi.riken.jp/FirstYear> (2010)
- [196] K. Hurley, *et al.*, Astrophys. J. Supp. submitted (2012)
- [197] J. Paul, *et al.*, arXiv:1104.0606 (2011)
- [198] A. Jung, *et al.*, arXiv:1106.3802 (2011)
- [199] G. W. Fraser, *et al.*, Proc. SPIE, **4497**, 115 (2002)
- [200] N. Gehrels, *et al.*, in IAU Symp, **285**, 41 (2012)
- [201] J. Camp, *et al.*, P.A.S.P., submitted (2012)
- [202] M. Feroci, *et al.*, Proc. SPIE, **7732**, 7732 (2010)
- [203] R. K. Manchanda, Proc 29th Astron. Soc. India, **3**, 53 (2011)